surements and the Microanalytical Service Unit, ANU.

Registry No. $[Co(diNOsar)]Cl_3$, 71935-78-9; $[Co(diNOsar)](CH_3CO_2)_3$, 91192-19-7; $[Co(diNOsar)](ClO_4)_3$, 91002-73-2; $[Co(diNOsar)](NO_3)_3$, 91002-74-3; $[Co(diNOsar)](CF_3SO_3)_3$, 91002-75-4; $[Co(NOsen)]Cl_3$, 91002-76-5; $[Coen_2(enim)]I_3$, 91002-77-6; $[Co(NMeNOsen)]Cl_3$, 91032-16-5; $[Co(diNOsar-H)]Cl_2 \cdot 4H_2O$, 91032-17-6; $[Co(diNOsar-H)](ClO_4)_2$, 91002-79-8; $[Co(diNOsar)](ClO_4)_2$, 71935-81-4; $[Co(diAMsar)]Cl_3$, 91002-80-1; $[Co(diAMsarH_2)]Cl_5$, 71935-72-3; $[Co(CLNOsar)]Cl_3$, 91002-81-2; $[Co(HONOsar)]Cl_3$, 91002-82-3; $[Co(diCLsar)]Cl_3$, 91002-83-4; $[Co(CLHOsar)]Cl_3$, 91002-84-5; $[Co(diHOsar)]Cl_3$, 91002-85-6; $[Co((ClMe)NOabsar)]Cl_3$, 91109-32-9; $[Co((ClMe)Clabsar)]Cl_3$, 91109-33-0; $[Co((Clme)HOabsar)]Cl_3$, 91109-34-1; $[Co(AM(Clme)absarH)]Cl_4$, 91032-18-7; $[Co(sar)]Cl_3$, 71935-73-4; $[Co(MENOsar)]Cl_3$, 91002-87-8; $[Co(AMMEsarH)]Cl_4$, 91002-88-9; $[Co(CLMEsar)]Cl_3$, 91002-89-0; $[Co(HOMEsar)]Cl_3$, 91002-90-3; $[Co(Clmeabsar)]Cl_3$, 91032-19-8; $[Co(en)_3]Cl_3$, 13408-73-6; $[Co(sen)]Cl_3$, 82796-46-1; HCHO, 50-00-0; CH_3NO_2, 75-52-5; diNOsar, 87655-55-8; diAMsar, 91002-72-1; AMMEsar, 91002-71-0.

Supplementary Material Available: A listing of positional and thermal parameters, hydrogen atom coordinates, and the observed and calculated structure amplitudes (17 pages). Ordering information is given on any current masthead page.

Cadmium-113 Shielding Tensors of Oxo Cadmium Compounds. 2. Single-Crystal Studies on Cadmium Calcium Tetraacetate Hexahydrate, Cadmium Maleate Dihydrate, Cadmium Formate Dihydrate, Cadmium Diammonium Disulfate Hexahydrate, and Cadmium Diacetate Dihydrate

Robert S. Honkonen and Paul D. Ellis*

Contribution from the Department of Chemistry, University of South Carolina, Columbia, South Carolina 29208. *Received December 8, 1983*

Abstract: Crystals of the title compounds have been investigated by single-crystal oriented ^{113}Cd NMR. The orientation of six distinct ^{113}Cd shielding tensors in the respective molecular reference frames has been determined. In each case, the tensor configuration was found to comply with the cadmium site symmetry. Tensor-lattice site orientations for cadmium calcium tetraacetate and cadmium maleate were unambiguously determined via NMR and crystallographic data. The ^{113}Cd NMR of cadmium formate, cadmium diammonium disulfate, and cadmium acetate crystals gave rise to symmetry-related tensors. A qualitative method for making symmetry-related tensor-lattice site assignments is introduced and was employed for these cadmium salts. The magnitude and orientation of the principal elements of the ^{113}Cd shielding tensor are discussed in terms of the structural features of the corresponding oxo cadmium reference frame and tensor element-structure correlations are proposed.

The importance of ^1H and ^{13}C NMR in organic and organometallic structure determination may be second only to X-ray crystallography. The utility of these nuclei as structural probes rests largely upon well-established isotropic chemical shift-structure correlations. Now, the demonstration of at least partial retention of activity for cadmium-substituted metalloproteins[1] coupled with the observation of ^{113}Cd resonances from cadmium-substituted metal-containing proteins[2-8] indicated that ^{113}Cd NMR and protein crystallography might enjoy a similar relationship with respect to the structure of the metal site in proteins. Specifically, native Ca^{2+} and Zn^{2+} could be replaced with NMR-favorable $^{113}Cd^{2+}$ and the metal coordination sphere configuration (the number and type of ligands) determined via comparison of the observed chemical shift with well-established shift-structure correlations. Unfortunately, the interpretation of isotropic shifts of spin $^1/_2$ metal nuclides in terms of structural parameters has not been straightforward.

Chemical shift data, solution and solid state, have demonstrated that specific regions within the nearly 1000-ppm ^{113}Cd shift range are dominated by particular ligand types.[8a,c] The overlap of these regions and the lack of intraregion relationships between σ_{iso} and the number of ligands, the cadmium-ligand distances, or the ligand type result in ambiguous shift-structure correlations. Hence, at the present time, cadmium thiolates[9] can be readily distinguished from oxo cadmium compounds; however, it is not possible to discriminate 6-, 7-, and 8-coordinate oxo complexes by employing only isotropic ^{113}Cd-shift data.[10] This deficiency clearly limits the utility of cadmium NMR as a structural tool.

Because of our present work in the application of ^{113}Cd NMR spectroscopy as a probe for calcium sites in troponin C[8d] we have been interested in a detailed understanding of the structural factors responsible for the shielding of the ^{113}Cd nucleus.[11] The sin-

(1) Vallee, B. L.; Ulmer, D. D. *Annu. Rev. Biochem.* **1972**, *19*, 591.
(2) Armitage, I. M.; Schoot-Uiterkamp, A. J. M.; Chlebowski, J. F.; Coleman, J. E. *J. Magn. Reson.* **1978**, *29*, 275.
(3) Drakenberg, T.; Lindman, B.; Cavé, A.; Parello, J. *FEBS Lett.* **1978**, *92*, 346.
(4) Forsén, S.; Thulin, E.; Lilja, H. *FEBS Lett.* **1979**, *104*, 123.
(5) Forsén, S.; Thulin, E.; Drakenberg, T.; Krebs, J.; Seamon, K. *FEBS Lett.* **1980**, *117*, 189.
(6) Sudmeier, J. L.; Bell, S. J.; Storm, M. C.; Dunn, M. F. *Science (Washington, D.C.)* **1981**, *212*, 560.
(7) Bailey, D. B.; Ellis, P. D.; Cardin, A. D.; Behnke, W. D. *J. Am. Chem. Soc.* **1978**, *100*, 5236.
(8) (a) Ellis, P. D. In "The Multinuclear Approach to NMR Spectroscopy"; Lamberg, J. B.; Riddell, F. B., Eds.; D. Reidel: Boston, 1982. (b) Armitage, I. M.; Otvos, J. O. *Biol. Magn. Reson.* **1982**, *4*, 79-144. (c) Ellis, P. D. *Science (Washington, D.C.)* **1983**, *221*, 4616. (d) Ellis, P. D.; Potter, J. D.; Strang-Brown, P. S. *J. Biol. Chem.*, submitted.
(9) Carson, G. K.; Dean, P. A. W.; Stillman, M. J. *Inorg. Chim. Acta* **1982**, *56*, 59.
(10) (a) Mennitt, P. G.; Shatlock, M. P.; Bartuska, V. J.; Maciel, G. E. *J. Phys. Chem.* **1981**, *85*, 2087. (b) Rodesiler, P. F.; Amma, E. L. *J. Chem. Soc., Chem. Commun.* **1982**, 182-184.
(11) Honkonen, R. S.; Doty, F. D.; Ellis, P. D. *J. Am. Chem. Soc.* **1983**, *105*, 4163.

0002-7863/84/1506-5488$01.50/0

Table I. Crystallographic Data and Cadmium Coordination Sphere Configuration of Oxo Cadmium Compounds

compd	ref	space group	unit cell parameters	coord no. and geom.	$\bar{d}$,[a] Δd,[b] and O ligand source
cadmium(II) maleate dihydrate	14	*Cc* (No. 9)[c]	a = 6.08 Å, b = 16.30 Å, c = 7.00 Å, Z = 4, 93.8°	6, distorted octahedron	$\bar{d}$ = 2.309; Δd = 0.297; 2 water, 2 bridging and 1 bidentate maleate
cadmium(II) diammonium disulfate hexahydrate	15	$P2_1/a$ (No. 14)[c]	9.43, 12.82, 6.29; Z = 2, 106.9°	6, octahedron	2.281; 0.057; 6 water
cadmium(II) formate dihydrate	16	$P2_1/c$ (No. 14)[c]	8.98, 7.39, 9.76; Z = 2, 97.3°	6, octahedron	2.271; 0.053; 6 bridging formate
				6, octahedron	2.289; 0.083; 4 water, 2 bridging formate
tricadmium(II) sulfate octahydrate	17	$C2/c$ (No. 16)[c]	14.78, 11.91, 9.47; Z = 4, 97.3°	6, octahedron	2.295; 0.009; 2 water, 4 monodentate sulfate
				6, octahedron	2.280; 0.071; 2 water, 4 monodentate sulfate
cadmium(II) diacetate dihydrate	18	$P2_12_12_1$ (No. 19)[c]	8.69, 11.92, 8.10; Z = 4	7, distorted square base–trigonal capped polyhedron	2.380; 0.303; 2 water, 2 bidentate and 1 bridging acetate
cadmium(II) calcium(II) tetraacetate hexahydrate	19	$I4/m$ (No. 87)[c]	$a = b$ = 11.37, c = 16.08; Z = 4	8, distorted dodecahedron	2.483; 0.388; 4 bidentate acetate
cadmium(II) dinitrate tetrahydrate	20	$Fdd2$ (No. 43)[c]	5.83, 25.86, 11.00; Z = 8	8, distorted dodecahedron	2.405; 0.333; 4 water, 2 bidentate nitrate

[a] Mean bond length in Å. [b] Bond length dispersion in Å. [c] Space group number. See ref 12c.

gle-crystal oriented NMR experiment[12] provides not only the principal elements of the shielding tensor but also the orientation of the elements within the molecular framework responsible for the observed chemical shift. This represents the most detailed structure–shift data available, and therefore the final approach that can be enlisted to establish chemical shift–structure correlations.

The purpose of the present work, in light of no readily discernible relation between coordination number or geometry and the isotropic shift, is to determine structure–tensor element correlations for a series of oxo cadmium compounds. The compounds we have investigated are $Cd(NO_3)_2 \cdot 4H_2O$, $3CdSO_4 \cdot 8H_2O$, $Cd\text{-}Ca(OAc)_4 \cdot 6H_2O$, $Cd(O_2CHCCHCO_2) \cdot 2H_2O$, $Cd(OAc)_2 \cdot 2H_2O$, $Cd(NH_4)_2(SO_4)_2 \cdot 6H_2O$, and $Cd_2(HCO_2)_4 \cdot 4H_2O$. The nitrate and sulfate data were reported earlier.[11] These crystals were chosen for several reasons. First, they represent simple examples of Cd(II) with an all-oxygen coordination sphere, a configuration consistent with metal sites in parvalbumin,[3] troponin C,[4] calmodulin,[5] insulin (calcium site),[6] and concanavalin A (S2 site).[7] Second, the series provides the opportunity to study 6-, 7-, and 8-coordinate cadmium. Finally, the crystals exhibit a normal distribution of space groups. The orientation of the shielding tensor occupying a variety of site symmetries can therefore be analyzed. Although this work is ^{113}Cd specific, the insight gained should be applicable to spin $^1/_2$ metal nuclides in general.

Experimental Section

Crystal Preparation. All crystals were obtained from aqueous solutions via controlled evaporation at room temperature. The cadmium formate and acetate salts were prepared by recrystallization of reagent grade salts. Cadmium calcium tetraacetate crystals were obtained from a saturated solution containing Cd(II), Ca(II), and Cu(II) acetates in mole ratios of 1:1:0.001. The trace Cu(II) was added to shorten the proton T_1's. Diffraction-quality crystals of the maleate salt were prepared by dissolving an excess of $Cd(OH)_2$ in a hot aqeuous solution of maleic acid. The cadmium Tutton salt,[13] $Cd(NH_4)_2(SO_4)_2 \cdot 6H_2O$, was recrystallized from an equimolar aqueous solution of $(NH_4)_2SO_4$ and $CdSO_4$. Crystals of sufficient volume (15–27 mm^3) were generally obtained without the need of a second seeding. Crystal parameters for the cadmium(II) maleate,[14] ammonium sulfate,[15] formate, [16] sulfate,[17] acetate,[18] calcium acetate,[19] and nitrate[20] salts are given in Table I.

Crystallographic Measurements. The orientation fo the unit cell with respect to the cube reference frame (see Data Analysis) was determined by crystallography. The orientation data for all crystals, excluding cadmium diammonium disulfate, were obtained by a combination of Weissenberg[21] and Laue[22] methods with Cu Kα radiation. The large crystal size (3 × 3 × 2 mm^3) coupled with the relatively large cadmium linear absorption coefficient for the Tutton salt made camera techniques difficult. Data, therefore, were obtained on an automated Enraf-Nonius CAD-4 diffractometer (Mo Kα radiation). Polymorphism and twinning were screened concurrently with the acquisition of orientation data. In all cases studied, we found the absence of high-angle twinning to be a sufficiently discriminating criterion for selecting crystals.

NMR Measurements. Data acquisition was via a standard matched Hartmann–Hahn[23] spin-locked cross-polarization[24] pulse sequence. Contact times were optimized in each case and varied from 1 to 10 ms. An acquisition time of 102.4 ms with a 4-s recycle time was uniformly employed. Typically, addition of 75–100 transients was required to achieve sufficient signal to noise ratios. Line widths were 2 and 6 ppm in the best and worst crystals, respectively. All experments were performed on a modified wide-bore WP-200 spectrometer which has been previously described.[25] Rotation of the crystals about an axis perpendicular to B_0 was accomplished by a goniometer system described elsewhere.[11]

Data Analysis. Mehring[12b] has given a delightfully straightforward treatment of the determination of Cartesian chemical shift–tensor elements in the crystallographic reference frame. We, therefore, only briefly review the essential features. A single crystal is fixed in a rigorously orthogonal cube. The unitary transformation matrix, **R**, relating the unit cell and the cube reference frames is determined via techiques mentioned above. The cube is subsequently mounted in a matching receptable that supports the crystal in the spectrometer. NMR spectra are taken at 10° increments for positive rotations about the three orthogonal cube axes. The typical sinusoidal rotation plot of chemical shift vs. rotation angle is obtained. The observed resonance shift depends solely upon the zz component of the shielding tensor in the laboratory frame, σ_{zz}^{lab}. In the secular approximation, the variation of a rank 2 tensor with orientation is given by the following expression:

$$\sigma_{zz}^{lab} = \tfrac{1}{2}(\sigma_{11}^{cube} + \sigma_{22}^{cube}) + \tfrac{1}{2}(\sigma_{11}^{cube} - \sigma_{22}^{cube}) \cos 2\theta - \tfrac{1}{2}(\sigma_{12}^{cube} + \sigma_{21}^{cube}) \sin 2\theta \quad (1)$$

where the rotation angle, θ, is about the three-axis of the cube frame.

(12) (a) Haeberlen, U. in "Advances in Magnetic Resonance", Supp. 1; Waugh, J. S., Ed.; Academic Press: New York, 1976. (b) Mehring, M. "High Resolution NMR Spectroscopy in Solids"; Springer-Verlag: New York, 1976. (c) "International Tables for X-ray Crystallography"; Kynoch Press: Birmingham, England, 1974; Vol. 1.

(13) Cadmium diammonium disulfate hexahydrate belongs to a group of ammonium sulfate double salts of divalent transition metals known as Tutton's salts; the Zn, Mg, Ni, Cu, and Cd salts are isomorphic.

(14) Hempel, A.; Hull, S. E. *Acta Crystallogr., Sect. B* **1979**, *B35*, 2215.

(15) Montgomery, H.; Lingafelter, E. C. *Acta Crystallogr.* **1966**, *20*, 728.

(16) Post, M. L.; Trotter, J. *Acta Crystallogr., Sect. B 1974*, *B30*, 1880.

(17) Richardson, J. W.; Jacobsen, R. A., personal communication.

(18) Harrison, W.; Trotter, J. *J. Chem. Soc., Dalton Trans.* **1972**, 956.

(19) Langs, D. A.; Hare, C. R. *Chem. Commun.* **1967**, 890.

(20) (a) Matkovik, B.; Ribar, B.; Zelenko, B. *Acta Crystallogr.* **1966**, *21*, 719. (b) Macdonald, A. C.; Sikka, S. K. *Ibid.* **1969**, *B25*, 1804.

(21) (a) Buerger, M. J. "X-ray Crystallography"; Wiley: New York, 1942. (b) Weissenberg, K. *Z. Phys.* **1924**, *23*, 229.

(22) Cullity, B. D. "Elements of X-ray Diffraction"; Addison-Wesley: Reading, MA, 1956; 215.

(23) Hartmann, S. R.; Hahn, E. L. *Phys. Rev.* **1962**, *128*, 2042.

(24) Pines, A.; Gibby, M. E.; Waugh, J. S. *J. Chem. Phys.* **1973**, *59*, 569.

(25) Inners, R. R.; Doty, F. D.; Garber, A. R.; Ellis, P. D. *J. Magn. Reson.* **1981**, *45*, 503.

Table II. Principal Elements of the ^{113}Cd Shielding Tensor and the Corresponding Direction Cosines Relating the PAS and the Crystallographic Unit Cell for $CdCa(OAc)_4 \cdot 6H_2O$

tensor element,[a] ppm		direction cosines			angle, deg		
		a	*b*	*c*	*a*	*b*	*c*
σ_{11}	-74.0	0.0115	-0.9998	0.0139	89	179	89
σ_{22}	-73.6	0.9999	0.0116	-0.0017	1	89	90
σ_{33}	101.2	-0.0019	0.0139	0.9999	90	89	1
$\bar{\sigma}^b$	-15.5						

[a] All shifts are reported relative to σ_{iso} for solid $Cd(ClO_4)_2$. [b] $\bar{\sigma} = {}^1/_3(\sigma_{11} + \sigma_{22} + \sigma_{33})$.

The rotation axis is required to be pendicular to B_0. Least-squares fitting of the laboratory response to this sinusoidal function for three rotation plots uniquely determines the six distinct elements of σ^{cube}. The resulting tensor is then transformed to the unit cell (crystal) reference frame via the general transformation

$$\sigma^{crystal} = \mathbf{R}\sigma^{cube}\mathbf{R}^{-1}$$

Diagonalization of $\sigma^{crystal}$ provides the desired eigenvalues and eigenvectors. The eigenvalues correspond to the principal elements (σ_{11}, σ_{22}, σ_{33}) of the shielding tensor and the eigenvectors to the direction cosines of the elements with respect to an orthogonal crystal reference frame.

Error Analysis. The error in the orientation of the shielding tensor in $CdCa(OAc)_4 \cdot 6H_2O$ can be estimated from data in Table II. Symmetry requires the unique element to be coincidental with the unique axis. σ_{33} makes an angle of 1° with *c*. This orientation, therefore, is good to within 1°. Similar arguments indicate an uncertainty of 1° in the cadmium maleate tensor orientation (Table IV). Estimates of the orientational error associated with the ^{113}Cd shielding tensors corresponding to cadmium in general lattice positions are obtained by comparing experimentally determined eigenvectors for a symmetry-related tensor with eigenvectors generated by applying the appropriate point group operator which relates the magnetically distinguishable lattice sites. The discrepancies are 3° and 2° for the cadmium acetate and cadmium diammonium disulfate crystals. The uncertainties for the cadmium formate crystal are 1° and 2° for the two distinct reference frames. The uncertainty in the eigenvalues is less than 3 ppm in all cases.

Theory

Six of the nine shielding tensors discussed in this paper correspond to cadmium nuclei in general positions within the respective unit cells. Hence, the assignment of symmetry-related tensors to the correct lattice sites is crucial.[26] We therefore remind the reader of the reason for assignment ambituities and, subsequently, treat the development of assignment criteria explicitly in this section.

Lattice sites related by point group symmetry operators are crystallographically equivalent and, in general, magnetically nonequivalent. The manifestation of this nonequivalence in the single-crystal experiment is the observation of distinguishable[27] shielding tensors arising from chemically and crystallographically equivalent lattice sites. The magnetic nonequivalence, therefore, results in assignment ambiguities. One must decide which set of eigenvectors belongs to which lattice site. Unfortunately, there is no single NMR experiment that can resolve this ambiguity. However, careful consideration of the definition of the shielding tensor suggests a method for assigning symmetry-related tensors.

The shielding tensor is defined as a second-order property of the atom of interest;[28] i.e.

$$\sigma_{\alpha\beta}^{A} = \left(\frac{\partial^2 E(\mu,B)}{\partial B_\beta \partial \mu_\alpha} \right)_{\mu=B=0} \quad (2)$$

Here, $E(\mu,B)$ is the total energy of the molecule with a magnetic moment on atom A in the presence of a uniform magnetic field

(26) For an extensive discussion of the relationship between crystallographic general positions and symmetry-related tensors see ref 11.

(27) Distinct tensors have different eigenvalues and, in general, different eigenvectors. A problem, however, occurs for symmetry-related tensors. Here, the eigenvalues are the same but the eigenvectors differ. If this difference is detectable we refer to the tensors as distinguishable.

(28) Ditchfield, R.; Ellis, P. D. In "Topics in C-13 NMR Spectroscopy"; Levy, G. C., Ed.; Wiley: New York, 1974; Vol. 1.

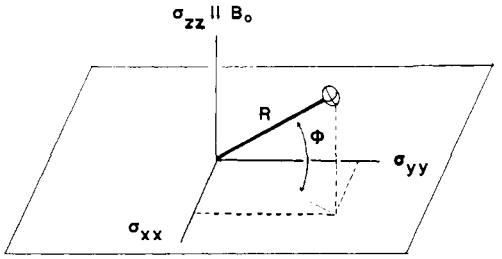

Figure 1. Geometrical details of the intramolecular shielding contribution, Θ_j^m, from a single bond to the *zz* component of the shielding tensor for nucleus *m*. The shielded nucleus is assumed to be at the origin with the ligand represented by the ellipse. See the text for further details.

B. The shielding tensor $\sigma_{\alpha\beta}^{A}$ (where $\alpha, \beta = x, y,$ or *z*) therefore represents the coupling between the α-component of the magnetic moment and the β-component of the induced field. In terms of molecular wave functions $\sigma_{\alpha\beta}^{A}$ is given as

$$\alpha_{\alpha\beta}^{A} = \left[\frac{\partial}{\partial B_\beta} \left\langle \Psi(B) \left| \frac{\partial H}{\partial \mu_\alpha} \right| \Psi(0) \right\rangle \right]_{\mu=B=0} \quad (3)$$

In eq 3 *H* is the total Hamiltonian for the molecule, and from the form of the operator it is easily seen that only terms that are linear in the magnetic moment are important within *H*. $\Psi(B)$ represents the perturbed wave function in the presence of the applied field. Independent of the various MO approximations that can be used to evaluate eq 3, the preceding equation can be written as a product of either charge density or current density matrix elements with dipole terms

$$\sigma_{\alpha\beta}^{A} = \sum_{\mu\nu} (P_{\mu\nu} \text{ or } j_{\mu\nu}) \left\langle \mu \left| \frac{O_p}{r^3} \right| \nu \right\rangle \quad (4)$$

In eq 4 $P_{\mu\nu}$ and $j_{\mu\nu}$ denote elements of the first-order density matrix or current density matrix, respectively. $\mu\nu$ are basis set atomic orbitals and Op denotes the appropriate operator.

Since the induced or local magnetic field has its origin in terms of current densities which are orthogonal to the induced field, eq 3 and 4 suggest that the *ii* component of the shielding tensor corresponding to nucleus *m* in the principal axis frame can be written as

$$\sigma_{ii}^{m} = \sum_j \frac{\Theta_j^m}{R_{mj}^3} \cos \phi_j \quad (5)$$

where the index *j* runs over all the atoms in the crystal (see Figure 1). Further, Θ_j^m denotes a parameter that describes the shielding contribution that atom *j* makes to atom *m*, R_{mj} is the distance between atom *j* and *m*, and ϕ_j is the angle between R_{mj} and the plane perpendicular to the *ii* component of the shielding tensor. In principal, there are on the order of 10^{24}–10^{25} terms that contribute to eq 5 and we can consider it to be an exact fitting expression. However, in practice, the sum converges with only a limited number of terms and eq 5 can be written in a more convenient form as

$$\sigma_{ii}^{m} = \sum_j \frac{\Theta_j^m}{R_{mj}^3} \cos \phi_j + \sum_{l \neq j} \frac{\Theta_l^m}{R_{ml}^3} \cos \phi_l + \sum_{k \neq l \neq j} \frac{\Theta_k^m}{R_{mk}^3} \cos \phi_k \quad (6)$$

Within the first sum in eq 6 the index *j* is limited to the atoms in the primary coordination sphere of atom *m*. The index in the second sum, *l*, runs over the remaining atoms in the lattice which contribute, significantly, to the overall sum. The final sum contains all remaining atoms in the crystal. This term will be ignored.

Equation 7 represents a more tractable form of eq 6. Here

$$\sigma_{ii}^{m} = \sum_L \Theta_L^m \sum_j \frac{\cos \phi_j}{R_{mj}^3} + \Theta^m \sum_{l'} \frac{\cos \phi_{l'}}{R_{ml'}^3} \quad (7)$$

we have made two approximations with respect to the second term.

First, the nonbonded shielding contribution Θ^m is considered to arise from pairwise interactions in a manner analogous to the bond susceptibility calculations of Flygare et al.[29] Consequently, $R_{ml'}$ is the distance between the shielded nucleus m and the center of the bond, l'. $\phi_{l'}$ represents the angle that the internuclear vector (between the atom pair constituting the bond) makes with the shielding plane perpendicular to σ_{ii}, the internuclear vector having been origin shifted to the nucleus. Second, Θ^m is, in general, considered to be independent of the atom types involved. Hence, we do not discriminate between C–O, S–O, and N–O pairwise interactions. This constraint is necessary to reduce the number of fitting parameters since we have, at most, three linearly independent fitting equations. One equation corresponds to each of the principle tensor elements. The nonbonded shielding contributions from the l' bond, therefore, is solely modulated by the geometric scaling factor $(\cos \phi_{l'})/R_{ml'}^3$. As in eq 6, the first term represents shielding contributions for atoms in the primary coordination sphere. The L index runs over ligand types, while j sums the scaling factors of all L-type ligands. Evaluating eq 7 for each tensor element and solving the resultant set of simultaneous equations provide values for each of the shielding contributors. Finally, comparing the values of the calculated shielding parameters provides a method for assigning symmetry-related tensors.

Bonded and nonbonded shielding contributions have been calculated for three cases (cadmium sulfate,[11] cadmium maleate, and cadmium calcium tetraacetate) where the tensor–lattice site assignements are unambiguous and a fourth, cadmium nitrate,[11] where the symmetry arguments are definitive. Omitting details which will be published subsequently, the following trends were noted: (1) bonded contributions from water oxygen, $\Theta(H_2O)$, fall in the deshielding range of $+750 \pm 250$ ppm Å^3, (2) nonbonded contributions are shielding relative to $\Theta(H_2O)$ with values ranging from -71 to 36 ppm Å^3, and (3) nitrate, sulfate, and maleate oxygens are found to have shielding contributions in the range of -800 ± 250 ppm Å^3. In all cases studied we have found that comparison of the signs of individual shielding contributions for possible tensor orientations is a sufficiently discriminating assignment criterion.

As an example, we provide the shielding contributions (ppm Å^3) as a function of ligand type for the two possible tensor orientations in the cadmium formate reference frame, Cd_w, containing four water and two formate oxygens.

	preferred orientation	nonpreferred orientation
$\theta(H_2O)$	947	−982
θ(formate)	−1092	−538
θ(nonbonded)	−59	236

The nonpreferred orientation is rejected because the negative water contribution indicates shielding relative to solid $Cd(ClO_4)_2$ and the positive nonbonded contribution indicates a relative deshielding influence. Both observations are inconsistent with the aforementioned data.

Results and Discussion

The shielding tensor configuration (i.e., symmetry and orientation relative to point group symmetry operators) is determined by the Cd site symmetry. Further, the tensor and lattice symmetries determine both the number of distinguishable tensors and also the orientational constraints imposed upon the shielding tensors.[30] Hence, the format for this section is an analysis of the tensor and lattice symmetries followed by a discussion of the tensor orientation in terms of structural features in the molecular reference frame. Six distinct ^{113}Cd shielding tensors have been determined, of which two, cadmium calcium tetraacetate and cadmium maleate, can be unambiguously assigned to the appropriate lattice site. Assignments of the symmetry-related tensors in the remaining crystals were based on the criteria discussed previously. The crystals involving unambiguous tensor–lattice site assignments are discussed first.

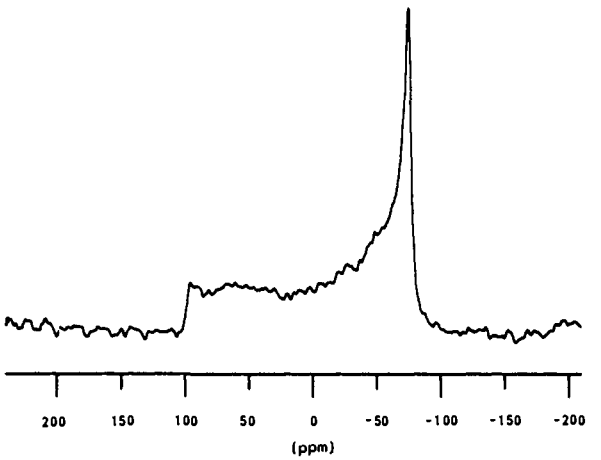

Figure 2. ^{113}Cd powder spectrum of $CdCa(OAc)_4 \cdot 6H_2O$ at 200 MHz. The shielding tensor is axially symmetric with $\sigma_{33} = 100$ ppm and $\sigma_{11} = \sigma_{22} = -75$ ppm. Chemical shifts are reported relative to solid $Cd(ClO_4)_2$.

$CdCa(OAc)_4 \cdot 6H_2O$. Cadmium calcium tetraacetate crystallizes in the $I4/m$ space group (see Table I). With the cadmium in special position, on the $\bar{4}(S_4)$, constraints are imposed upon both the tensor symmetry and orientation. The ^{113}Cd powder spectrum at 200 MHz is shown in Figure 2. As anticipated from the $\bar{4}$ site symmetry, the shielding tensor is seen to have rigorous axial symmetry. Additionally, the site symmetry fixes the orienation of the shielding tensor in the tetragonal reference frame. The principal elements are required to be coincidental with the unit cell axes, with the unique element, σ_{33}, further constrained to be aligned along c, the $\bar{4}$ axis. In this configuration the tensor orientations generated by the point group symmetry operators (C_4, m_c) are magnetically equivalent. The alignment of the unique element with the crystallographic rotation axis ensures rotational invariance for the C_4-related tensor. Also, the point group mirror is perpendicular to c and σ_{33}. Mirror-related tensors, therefore, are magnetically indistinguishable. Symmetry, therefore, requires a single distinguishable shielding tensor with the unique principal element aligned along c. Experimentally, a single line was indeed observed in each spectrum for rotation about the required orthogonal axes. The ^{113}Cd shielding tensor and the corresponding direction cosines are given in Table II, where σ_{33} is seen to have the appropriate orientation. It is interesting to note that the tetragonal crystal morphology was sufficiently well developed to allow orientation of the crystal such that the tensor PAS and the cube reference frame were congruent. For rotation about c, σ_{zz}^{lab} showed no angular dependence. Each spectrum contained a single resonance at −74 ppm. Rotations about the two remaining axes resulted in typical sinusoidal rotation plots with an interesting feature. The orientation corresponding to $\theta = 0°$ resulted in spectra with resonances at −74 and 101 ppm, for rotation axes a and b, respectively. This is expected from consideration of eq 1.

The cadmium coordination geometry in this double salt has been described by Langs and Hare[19] as a distorted dodecahedron. Details of the Cd-coordination geometry are found in Table III. Reference to Figure 3 reveals several conspicuous symmetry-imposed structural features. The Cd-coordination sphere consists of four pairs of $\bar{4}$-related bidentate acetate oxygens (see figure

(29) Schmalz, T. G.; Norris, C. L.; Flygare, W. H. *J. Am. Chem. Soc.* **1973**, *95*, 7961.

(30) (a) Weil, J. A.; Buch, T.; Clapp, J. E. *Adv. Magn. Reson.* **1973**, *7*, 183. (b) Nye, J. F. "Physical Properties of Crystals"; Oxford University Press: London, 1957. (c) Sands, D. E. "Tensors and Vectors in Crystallography"; Addison-Wesley: Reading, MA, 1982. (d) Gaylord, T. K. *Am. J. Phys.* **1975**, *43*, 861. (e) Schonland, D. S. *Proc. Phys. Soc., London, Sect. A* **1959**, *73*, 788.

(31) (a) Johnson, C. K. "ORTEP II"; Report ORNL-3794, Oak Ridge National Laboratory, Oak Ridge, TN, 1970. (b) "The X-Ray System"; Technical Report TR-455. Program LSQPL; Steward, J. M., Ed.; Computer Science Center, University of Maryland, College Park, MD, 1979.

Table III. Structural and Orientational Data for $CdCa(OAc)_4 \cdot 6H_2O$: Selected Internuclear Distances and Angles for the Cadmium Coordination Sphere and Details of the Orientation of the Principal Elements of ^{113}Cd Shielding Tensor in the Molecular Reference Frame

bond distances, Å		bond angles, deg		tensor element–ligand angle, deg	
Cd–O(1)		O(2)–Cd–O(4)	167	σ_{11}–Cd–O(3)	63
Cd–O(2)	2.289				
Cd–O(3)		O(3)–Cd–O(4)	91	σ_{11}–Cd–O(4)	152
Cd–O(4)		O(3)–Cd–O(1)	167	σ_{11}–Cd–O(6)	119
		O(3)–Cd–O(5)	97	σ_{11}–Cd–O(7)	78
Cd–O(5)		O(3)–Cd–O(8)	50	σ_{11}–Cd–O(8)	76
Cd–O(6)	2.676				
Cd–O(7)		O(4)–Cd–O(5)	117	σ_{22}–Cd–O(2)	116
Cd–O(8)		O(4)–Cd–O(6)	50	σ_{22}–Cd–O(3)	27
		O(4)–Cd–O7)	94	σ_{22}–Cd–O(5)	103
Cd–Ca	4.021			σ_{22}–Cd–O(8)	60
		O(5)–Cd–O(8)	135		
				σ_{33}–Cd–O(2)	84
				σ_{33}–Cd–O(3)	96
				σ_{33}–Cd–O(5)	34
				σ_{33}–Cd–O(6)	33

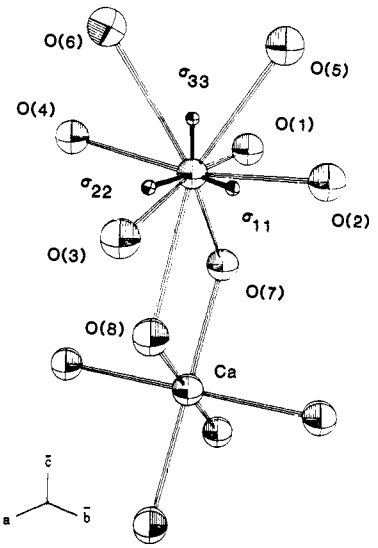

Figure 3. ORTEP[31a] illustrating the orientation of the principal elements of the shielding tensor within the molecular reference frame for $CdCa(OAc)_4 \cdot 6H_2O$. Acetate carbons are not shown for clarity. O(2) and O(5) belong to the same acetate as do O(3) and O(8). Details are found in Table III.

caption for details). The Cd–O bond lengths are equally divided between 2.289 and 2.676 Å, with O(5) through O(8) being significantly longer. Also, O(1) through O(4) are alternately positioned 6° below and above the best least-squares plane (BLP)[31b] containing O(1), O(2), O(3), O(4), and Cd.

The orientation of the ^{113}Cd shielding tensor in the molecular reference frame is illustrated in Figure 3 and detailed in the last column of Table III. The dominant orientational feature is the position of σ_{33} (101 ppm), distinctly the least shielded element. σ_{33} is rigorously orthogonal to the BLP containing the short-bond oxygens and Cd. As discussed above, σ_{33} is coincidental with c and necessarily bisects the O(5)–Cd–O(6) and O(7)–Cd–O(8) angles (66°). Considering O(1)–O(4) and O(5)–O(8) to be the short- and long-bond oxygens, respectively, the intramolecular shielding contributions to σ_{33} (i.e., to the shielding plane normal to σ_{33}) are clearly dominated by the short-bond oxygens. Because of the highly symmetric ligand geometry this is conveniently understood in terms of the following factors. First, the Cd–short-bond oxygen internuclear vectors make acute angles of 6° with the shielding plane normal to σ_{33} compared to angles of 57° for the Cd–long-bond oxygen vectors. The short-bond oxygen contribution is therefore scaled by 0.995 (cos 6°), compared to 0.545 for the long-bond contribution (see eq 7). Second, the large bond length difference (0.388 Å) results in R^{-3} scaling factors, 0.083 and 0.052, which again favors the short-bond oxygen shielding contribution. The shielded elements, σ_{11} and σ_{22}, lie in the short-bond oxygen–Cd BLP, with σ_{22} oriented 67°, 70°, and 63° from the O(5)–Cd–O(6) BLP, O(2)–Cd–O(6) BLP, and the O(2)–Cd–O(4) best least-squares line (BLL), respectively. The more general orientation of the shielded elements results in roughly comparable short- and long-bond oxygen intramolecular shielding contributions, with the long-bond contributions being slightly larger.

Table IV. Principal Elements of the ^{113}Cd Shielding Tensor for Cadmium Maleate Dihydrate. Eigenvectors and Corresponding Angles are with Respect to the Orthogonal $a'bc'$ Unit Cell[a]

tensor element,[b] ppm		eigenvectors (direction cosines)			angle, deg		
		a'	b	c'	a'	b	c'
σ_{11}	−46.8	0.8012	−0.0055	−0.5983	37	90	127
σ_{22}	3.8	0.5984	0.0126	0.8011	53	89	37
σ_{33}	73.2	−0.0031	0.9999	−0.0134	90	1	91
$\bar{\sigma}$	10.4						

[a] For a discussion of the orthogonalization of monoclinic reference frames see ref 11. [b] Chemical shifts reported relative to solid $Cd(ClO_4)_2$.

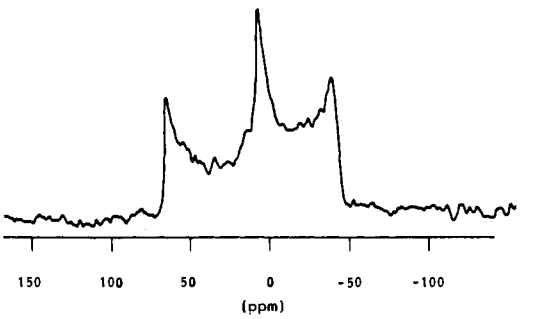

Figure 4. Nonaxial (η = 0.70) ^{113}Cd powder spectrum of cadmium maleate dihydrate recorded at 200 MHz. The discontinuities occur at −47, 4, and 73 ppm relative to $\bar{\sigma}$ for solid $Cd(ClO_4)_2$.

$Cd(C_4H_2O_4) \cdot 2H_2O$. Two monoclinic structures of cadmium maleate dihydrate have been reported. Post and Trotter[32] solved the initial structure in the $P2_1/c$ space group. Hempell, Hull, Ram, and Gupta reported a second polymorph in space group Cc. In our hands the Cc form (Table I) is favored. The single-crystal experiment was performed on this form. The general equivalent positions for Cc are $x, y, z; x, \bar{y}, z + {}^1/_2$. Hence, two orientations for the shielding tensor with respect to the point group mirror must be considered. The tensor may have a principal axis normal to the mirror plane (i.e., coincidental with b), in which case a single resonance is expected for all orientations of the crystal. Alternatively, the principal elements may have general orientations with respect to m_b. In this configuration, the crystallographically equivalent positions are magnetically inequivalent for general orientations of the crystal relative to B_0 and two resonances of equal intensity result. Experimentally, all spectra contained a single line. Note the alignment of σ_{33} with b in Table IV. The single distinguishable ^{113}Cd shielding tensor was determined and found to have three distinct principal elements (−46.8, 3.8, and 73.2 ppm) which are in good agreement with the discontinuities observed in the powder spectrum (Figure 4). It is interesting to note that the structure was solved with Cd in general position. The corresponding C_1 site symmetry imposes no orientational constrains upon the shielding tensor. A priori, therefore, one would have anticipated two distinguishable tensors with three principal shielding directions having completely general orientations with m_b.

The cadmium coordination sphere is illustrated in Figure 5 and the corresponding structural details are found in Table V. The

(32) Post, M. L.; Trotter, J. *J. Chem. Soc., Dalton Trans.* **1974**, 674.

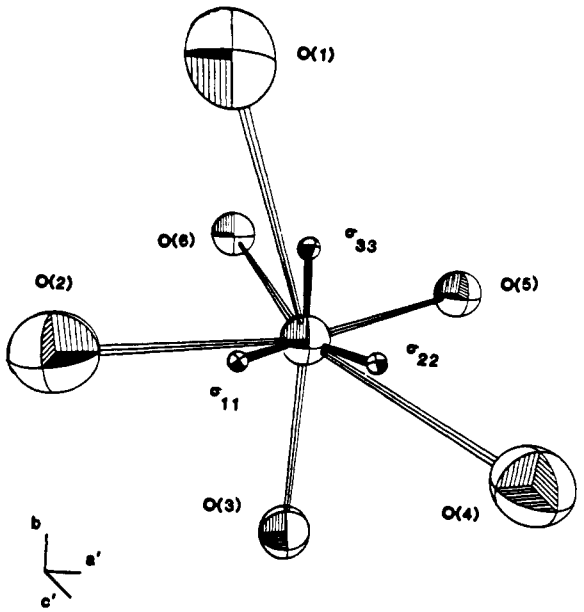

Figure 5. Illustration of the location of the principal elements of the ^{113}Cd shielding tensor within the cadmium coordination sphere for cadmium maleate dihydrate. O(5) and O(6) are water oxygens. O(1) and O(2) are oxygens of the same bidentate maleate, whereas O(3) and O(4) belong to separate bridging maleates.

Table V. Bond Distances and Angles for $Cd(C_4H_2O_4)\cdot 2H_2O$ and Details of the Orientation of the Principal Elements of the ^{113}Cd Shielding Tensor in the Molecular Reference Frame

bond distances, Å		bond angles, deg		tensor element–ligand angles, deg	
Cd-O(1)	2.521	O(1)-Cd-O(2)	54	σ_{11}-Cd-O(1)	62
Cd-O(2)	2.245	O(1)-Cd-O(3)	146	σ_{11}-Cd-O(2)	10
Cd-O(3)	2.224	O(1)-Cd-O(4)	90	σ_{11}-Cd-O(3)	85
Cd-O(4)	2.326	O(1)-Cd-O(5)	110	σ_{11}-Cd-O(4)	88
Cd-O(5)	2.247	O(1)-Cd-O(6)	90	σ_{11}-Cd-O(5)	167
Cd-O(6)	2.291			σ_{11}-Cd-O(6)	109
		O(2)-Cd-O(3)	94		
		O(2)-Cd-O(4)	95	σ_{22}-Cd-O(1)	81
		O(2)-Cd-O(6)	100	σ_{22}-Cd-O(2)	96
				σ_{22}-Cd-O(3)	90
		O(3)-Cd-O(4)	79	σ_{22}-Cd-O(4)	12
		O(3)-Cd-O(5)	101	σ_{22}-Cd-O(5)	78
		O(4)-Cd-O(5)	137	σ_{22}-Cd-O(6)	153
		O(5)-Cd-O(6)	81		
				σ_{33}-Cd-O(1)	30
				σ_{33}-Cd-O(2)	81
				σ_{33}-Cd-O(3)	175
				σ_{33}-Cd-O(4)	101
				σ_{33}-Cd-O(5)	84
				σ_{33}-Cd-O(6)	71

coordination sphere is a highly distorted octahedron through a pair of water oxygens, O(5) and O(6), two bridging maleate oxygens, O(3) and O(4), and two oxygens from a bidentate maleate, O(1) and O(2). Six distinct Cd–O bond distances range from 2.224 to 2.521 Å, with the Cd-OH_2 distances being intermediate. Figure 5 illustrates the orientation of the principal shielding directions with respect to the molecular reference frame. The tensor element–ligand geometry is given in the last column of Table V. If O(1) and O(3) are considered axial positions, then the equatorial plane contains Cd, O(2), O(4), and the water oxygens, O(5) and O(6). With this in mind, the more shielded elements, σ_{11} and σ_{22}, are oriented 11° from the equatorial BLP. σ_{11}, the most shielded element, is directed 77° from the O(1)–Cd–O(4) BLP, making angles of 62 and 88° with the Cd–O(1) and Cd–O(4) internuclear vectors, respectively. Conversely, the σ_{22}–O(1)–Cd–O(4) BLL angle is 15° with σ_{22}–Cd–O(1) and σ_{22}–Cd–O(4) angles of 81° and 12°. The "more orthogonal" orientation of the most shielded element with respect to the plane

Table VI. Principal Elements of the ^{113}Cd Shielding Tensors and Corresponding Direction Cosines Assigned to Cadmium in the Cd_w and Cd_f Reference Frames of Cadmium Formate Dihydrate

tensor element, ppm		direction cosines[a]			angles, deg		
		a'	b'	c'	a'	b'	c'
			Cd_w				
σ_{11}	−55.8	−0.9432	0.0719	0.3242	160	80	71
σ_{22}	30.3	0.3319	0.2432	0.9114	71	76	24
σ_{33}	85.1	0.0133	−0.9673	0.2533	89	165	75
$\bar{\sigma}$[b]	19.9						
			Cd_f				
σ_{11}	−18.8	−0.0014	−0.2046	0.9789	90	102	12
σ_{22}	17.4	−0.4014	−0.8964	−0.1879	114	154	101
σ_{33}	45.6	0.9159	−0.3932	−0.0808	24	113	95
$\bar{\sigma}$	14.7						

[a] The primed axis system represents the orthogonalized monoclinic unit cell.[11] [b] $\bar{\sigma} = {}^1/_3$ Tr (σ).

defined by the longest Cd–O bonds is consistent with data reported for cadmium sulfate and nitrate.[11] σ_{33} is oriented 81°, 101°8 84°, and 71° from the equatorial Cd–O vectors. The resulting σ_{33}–equatorial BLP angle is 80°. The nearly perpendicular orientation of the least shielded element relative to the plane containing the water oxygens should be noted.

$Cd_2(HCO_2)_4\cdot 4H_2O$. Cadmium formate dihydrate crystals belong to the $P2_1/c$ space group and consequently the $2/m$ point group. Post and Trotter solved the crystal structure with two independent cadmium in the asymmetric unit (Table I). With $Z = 2$ there are four Cd per unit cell. One pair corresponds to each independent lattice position. All Cd atoms are on space group special positions occupying centers of symmetry. The two independent cadmium are six-coordinate: Cd_w through four water and two formate oxygens and Cd_f through formate oxygens exclusively. Since the shielding tensors of the symmetry-related cadmiums transform under the $2/m$ point group operators (xyz, $\bar{x}\bar{y}\bar{z}$; $\bar{x}y\bar{z}$, $x\bar{y}z$), only two distinguishable tensors corresponding to Cd_w with eigenvectors related by the point group twofold are expected. Note that each pair of operators is related by a center of inversion which is not detected by the NMR experiment. Further, the Cd_w site symmetry ($\bar{1}$) imposes no orientational or symmetry constraints upon the tensors. The principal elements of the ^{113}Cd shielding tensor and the corresponding direction cosines are found in Table VI. A single set of direction cosines is reported for the tensors corresponding to cadmium in the water-containing frame. The eigenvectors for the second tensor are generated by the twofold along b. As anticipated, the eigenvalues and eigenvectors corresponding to Cd_w indicate an asymmetric tensor (three distinct elements), assuming a general orientation with respect to the crystallographic reference frame. Identical arguments can be forwarded to account for both the tensor configurations and the number of distinguishable tensors associated with Cd_f sites.

The CP-MAS spectrum of cadmium formate contains two resonances (14 and 20 ppm) of comparable intensity for a contact time of 5 ms.[23,24,33] This is, of course, consistent with equivalent occupancy of the two chemically and crystallographically distinct sites, Cd_w and Cd_f. The assignment of the less shielded resonance (20 ppm) to the Cd_w site was based upon the r_{CdH}^{-3}, dependence of the intensity of a resonance generated by a matched Hartmann–Hahn spin-locked cross-polarization pulse sequence. For a given contact time, the enhancement of the observed ^{113}Cd resonance depends upon the rate of the resonant cross relaxation between ^{113}Cd and ^1H, T_{CdH}^{-1}. Now, T_{CdH}^{-1} depends primarily upon the ^{113}Cd–^1H dipolar coupling which, in turn, is directly proportional to r_{CdH}^{-3}, where r_{CdH} is the internuclear distance. The enhancement of the 20-ppm line relative to the resonance at 14 ppm for short contact times (0.1–1 ms) provided an unambiguous assignment of this resonance and the tensor with eigenvalues of

(33) Schaefer, J.; Stejskal, E. O.; Buchdahl, R. *Macromolecules* **1975**, *8*, 291.

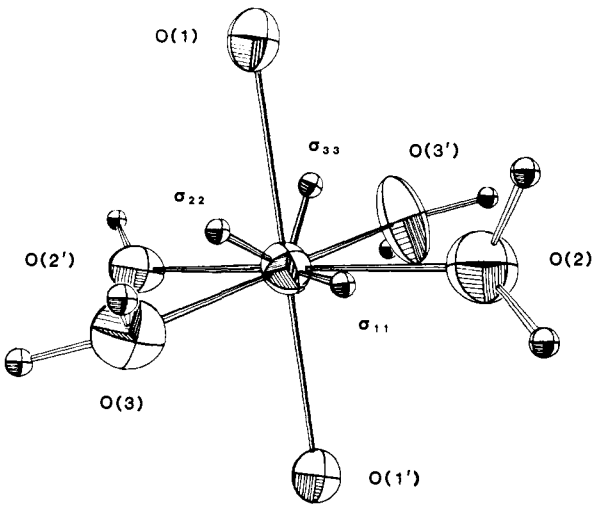

Figure 6. ORTEP indicating the orientation of the principal elements of ^{113}Cd shielding tensor with respect to the Cd_w lattice site in cadmium formate. Primed labels indicate inversion-related atoms. Protons are not labeled for clarity. O(1) and O(1′) are bridging formate oxygens.

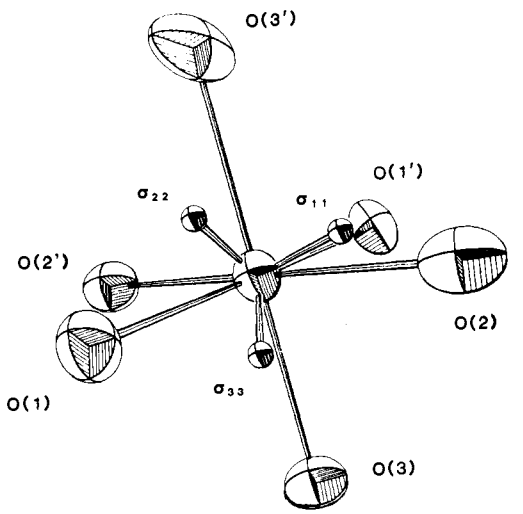

Figure 7. Preferred orientation of the ^{113}Cd shielding tensor in the Cd_f reference frame of the cadmium formate dihydrate crystal. Primed labels indicate inversion center-related atoms. All oxygen ligands are from bridging monodentate formates.

Table VII. Geometrical Data for Cadmium Formate: Bond Distances and Angles for the Cd_w Coordination Sphere and Details of the Orientation of the Principal Shielding Directions in the Molecular Reference Frame

bond distances, Å		bond angles, deg		tensor element–ligand angles, deg	
Cd–O(1)	2.326	O(1)–Cd–O(1′)	180	σ_{11}–Cd–O(1)	87
Cd–O(2)	2.298	O(1)–Cd–O(2)	87.5	σ_{11}–Cd–O(1′)	93
Cd–O(3)	2.242	O(1)–Cd–O(3)	89.6	σ_{11}–Cd–O(2)	6
				σ_{11}–Cd–O(3)	84
		O(2)–Cd–O(3)	90.1		
				σ_{22}–Cd–O(1)	54
				σ_{22}–Cd–O(2)	95
				σ_{22}–Cd–O(3)	36
				σ_{33}–Cd–O(1)	36
				σ_{33}–Cd–O(2)	87
				σ_{33}–Cd–O(3)	126

Table VIII. Structural Data for Cadmium Formate: Interatomic Distances and Angles for the Primary Cd_f Coordination Sphere and Details of the Tensor–Ligand Geometry

interatomic distances, Å		interatomic angles, deg		tensor element–ligand angles, deg	
Cd–O(1)	2.248	O(1)–Cd–O(1′)	180	σ_{11}–Cd–O(1)	107
Cd–O(2)	2.263	O(1)–Cd–O(2)	91	σ_{11}–Cd–O(1′)	73
Cd–O(3)	2.300	O(1)–Cd–O(3)	93	σ_{11}–Cd–O(2)	25
				σ_{11}–Cd–O(3)	105
		O(2)–Cd–O(3)	88		
				σ_{22}–Cd–O(1)	48
				σ_{22}–Cd–O(2)	92
				σ_{22}–Cd–O(3)	140
				σ_{33}–Cd–O(1)	47
				σ_{33}–Cd–O(2)	65
				σ_{33}–Cd–O(3)	54

−55.8, 30.3, and 85.1 to the proton-rich Cd_w frame.[34] Note that one-third the sum of the Cd_w eigenvalues gives the isotropic shift. This assignment might have been expected from the deshielding influence of water ligands. Also, the larger anisotropy reflects the ligand asymmetry in the Cd_w coordination.

The orientation of the shielding tensor in the Cd_w reference frame is illustrated in Figure 6. The Cd_w coordination sphere geometry and tensor–ligand geometry are detailed in Table VII. Referring to Figure 6, one can see the Cd_w coordination sphere to be an axially distorted octahedron via two bridging formate and four water oxygens. The Cd–O distances are uniform (2.242–2.326 Å), with the Cd–$OCHO^-$ distance being slightly longer. Two structural features are significant: (1) the axial positions of O(1) and O(1′), and (2) the equatorial plane consisting of water oxygens O(2), O(2′), O(3), and O(3′). The orientation of the principal shielding directions relative to the axial BLL and the equatorial BLP demonstrates characteristic features. The most shielded element, σ_{11}, is oriented 87° from the axial BLL, making angles of 87° and 93° with the longest Cd–O internuclear vectors, Cd–O(1) and Cd–O(1′). σ_{11} is concomitantly oriented 87° from the normal to the equatorial BLP. In addition, the least shielded element, σ_{33}, makes the largest acute angle (54°) with the equatorial BLP. The σ_{22} angle is necessarily the σ_{33} complement. The larger deshielding contribution of the water plane to σ_{33} is reflected in the magnitudes of the eigenvalues.

(34) Cd_w has six protons within 3 Å. The Cd_f sphere of the same radius is devoid of protons.

The Cd_f-coordination sphere is illustrated in Figure 7 and detailed in Table VIII. The coordination geometry is again a distorted octahedron; however, the six coordinated formate oxygens provide a symmetric reference frame with respect to ligand type. Additionally, the Cd_f–O bond distances are slightly more uniform than the Cd_w–O distances, varying from 2.248 to 2.300 Å. The orientation of the ^{113}Cd shielding tensor in the highly symmetric Cd_f frame is seen in Figure 7. Details are given in the final column of Table VIII. The principal shielding directions assume general orientations relative to the axial BLL, O(3)–Cd–O(3′), and the equatorial BLP containing the shorter Cd–O bonding distances. In this configuration, the shielding environment normal to the principal elements represents the sum of significant shielding contributions from each Cd–OHCO– interaction. Definite correlations between tensor elements and individual structural parameters (i.e., extreme bonding distances, short-bond planes, or water-containing planes) are, therefore, not possible. The tensor orientation can, however, be understood within the context of the formalism employed to assign the symmetry-related eigenvectors to this site. As indicated in the Theory section, the shielding contribution due to an isolated Cd–OCHO– interaction is scaled by $(\cos \phi)/R^3$. The sum of the six scaling factors, one corresponding to each pairwise interaction, is therefore proportional to that net intramolecular shielding contribution to the corresponding tensor element. Hence, a comparison of the three scaling factors should reflect the tensor elements trend to lesser shielding. The calculated scaling factors are 0.199, 0.203, and 0.208 $Å^{-3}$ for $\sigma_{11} = -18.8$, $\sigma_{22} = 17.4$, and $\sigma_{33} = 45.6$, respectively. Increasing scaling factors corresponding to increasing eigenvalues is consistent

Table IX. Principal Elements of the ^{113}Cd Shielding Tensor and Corresponding Direction Cosines for $Cd(NH_4)_2(SO_4)_2 \cdot 6H_2O$

tensor element,[a] ppm		direction cosines			angles, deg		
		a'	b	c'^b	a'	b	c'^b
σ_{11}	13.7	0.3630	0.4466	−0.8178	69	63	145
σ_{22}	70.1	−0.4726	0.8446	0.2514	118	32	75
σ_{33}	97.9	0.8030	0.2952	0.5177	37	73	59
$\bar{\sigma}^c$	60.6						

[a] Shifts are reported relative to solid $Cd(ClO_4)_2$. [b] The primed axis system represents the orthogonalized monoclinic unit cell axes. [c] $\bar{\sigma} = {}^1/_3$ Tr (σ).

Table X. Structural Data for Cadmium Ammonium Sulfate Hexahydrate: Selected Interatomic Distances and Angles[a] for the Cadmium Coordination Sphere and Details of the ^{113}Cd Shielding Tensor Orientation within the Molecular Frame

interatomic distances, Å		interatomic angles,[a] deg		tensor element–ligand angle,[a] deg	
Cd–O(1)	2.247	O(1)–Cd–O(1′)	180	σ_{11}–Cd–O(1)	159
Cd–O(2)	2.297	O(1)–Cd–O(2)	91	σ_{11}–Cd–O(1′)	21
Cd–O(3)	2.298	O(1)–Cd–O(3)	93	σ_{11}–Cd–O(2)	101
				σ_{11}–Cd–O(3)	70
		O(2)–Cd–O(3)	89		
				σ_{22}–Cd–O(1)	98
				σ_{22}–Cd–O(2)	16
				σ_{22}–Cd–O(3)	75
				σ_{33}–Cd–O(1)	70
				σ_{33}–Cd–O(2)	101
				σ_{33}–Cd–O(3)	25

[a] Angles involving prime labeled atoms are the supplements of the unprimed counterparts.

with a deshielding contribution (relative to $Cd(ClO_4)_2$) for the formate oxygens. This is in agreement with the deshielded isotropic shift of 17.4 ppm.

Since the tensor–lattice site assignment was based on the same formalism employed to develop a rationale for the tensor orientation, the potential for circular reasoning should be noted. Fortunately, the alternative assignment can be discounted on independent grounds. Referring to Figure 7, one finds that the alternative assignment aligns σ_{22} with the Cd–O(2′) vector and concomitantly places σ_{11} and σ_{33} in the O(3′), O(1), O(3), O(1′) plane, making angles of 46° and 45°, respectively, with the Cd–O(3′) vector. This orientation results in the most shielded and deshielded elements having similar orthogonal environments. This is clearly an unreasonable configuration.

$Cd(NH_4)_2(SO_4)_2 \cdot 6H_2O$. The crystal structure of the cadmium Tutton salt[13] was solved by Montgomery and Lingafelter. The crystals have monoclinic Laue symmetry, point group $2/m$. See Table I for crystal details. The refinement was done with Cd on the space group ($P2_1/a$) special position. The point group operators (xyz, $\bar{x}\bar{y}\bar{z}$; $\bar{x}y\bar{z}$, $x\bar{y}z$) therefore generate only two magnetically distinguishable sites. In addition, the $\bar{1}$ site symmetry imposes no constraints on the shielding tensor configuration. Two distinguishable shielding tensors with three distinct principal elements are therefore expected. All rotation spectra contained two resonances from which two tensors were determined. The ^{113}Cd shielding tensor elements and corresponding direction cosines are given in Table IX. As anticipated, the tensor has three distinct elements, assuming general orientations relative to the unique axis, b. As before, only one set of eigenvectors is reported.

An ORTEP illustrating the primary coordination in the Tutton salt reference frame is seen in Figure 8. Details of the coordination geometry are found in Table X. The cadmium ion, which lies on a center of symmetry, is surrounded by a slightly distorted octahedron of water molecules. Table X shows the axial bonds, Cd–O(1) and –O(1′), to be 0.05 Å shorter than the equatorial bonds, Cd–O(2), Cd–O(2′), Cd–O(3), Cd–O(3′). The maximum deviation from octahedral angles is 3°. Hence, the idealized molecular symmetry is D_{4h}. With this in mind, the $\eta = 0.59$ tensor

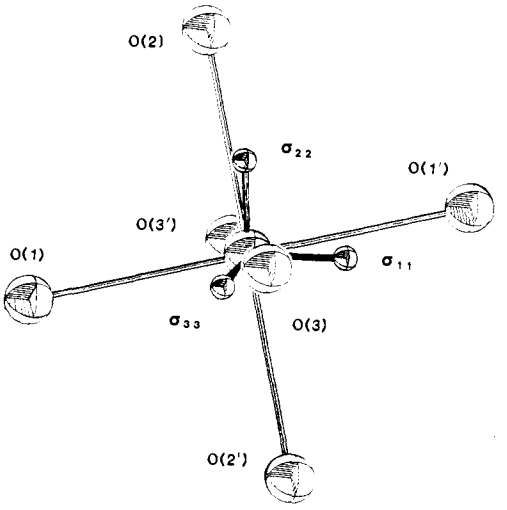

Figure 8. ORTEP depicting the orientation of the ^{113}Cd shielding tensor in the hexaaquocadmium Tutton salt reference frame. Primed labels indicate center of inversion-related atoms.

symmetry demonstrates the tensor configuration compliance with the nuclear site symmetry and not the molecular symmetry. While the intramolecular shielding contribution invariably reflects the small deviation from D_{4h} symmetry, the large difference from an $\eta = 0$ tensor suggests that the intramolecular shielding contribution may be significant.

The sole asymmetric structural feature of the cadmium Tutton salt reference frame is the shorter axial bonds, Cd–O(1) and Cd–O(1′). Short bond–deshileding correlations were found in the $CdCa(OAc)_4 \cdot 6H_2O$ and the $Cd_2(HCOO)_4 \cdot 4H_2O$ (Cd_f site) crystals. The significant feature of the tensor orientation is the location of σ_{11} (Figure 8). The most shielded element is oriented 21° from the axial BLL, making angles of 21° and 159° with the Cd–O(1′) and Cd–O(1) vectors. Conversely, the deshielded elements make axial BLL angles of 82 and 70° for σ_{22} and σ_{33}, respectively. Recall that the tensor element reflects current density in the plane normal to the direction of the element. The considerably smaller short-bond contribution to the shielded element relative to the deshielded elements is consistent with the 56- and 84-ppm difference in the eigenvalues (Table IX). An additional feature to be noted is the comparable environments orthogonal to σ_{22} and σ_{33}. σ_{22} is directed 74° from the O(1), O(3), O(1′), O(3′), Cd BLP, making angles of 82° and 75° with the Cd–O(1) and Cd–O(3) vectors. The σ_{33}–Cd–O(1) and σ_{33}–Cd–O(2) angles are 70° and 101°, resulting in an O(1), O(2′), O(1′), O(2), Cd BLP angle of 68°. Since σ_{22} and σ_{33} differ by 28 ppm relative to an anisotropy of 84 ppm, this configuration is quite reasonable. The "more orthogonal" orientation of σ_{22} with respect to the appropriate water-containing plane should be noted. This would appear to indicate that σ_{22} should be the more deshielded of the two elements. The apparent contradiction is clarified by including the respective axial water contributions and comparing the net scaling factors for the intramolecular shielding contribution. The scaling factors are 0.382 and 0.402 $Å^{-3}$ for σ_{22} and σ_{33}, which is consistent with σ_{33} having the most deshielded eigenvalue.

The alternative tensor–lattice site assignment corresponds to a C_2 rotation about b. This can be qualitatively visualized in Figure 8 by switching the labels on σ_{11} and σ_{33}. This assignment, however, results in similar orthogonal environments for the most shielded and deshielded elements.

$Cd(OAc)_2 \cdot 2H_2O$. Cadmium acetate crystals are orthorhombic in the space group $P2_12_12_1$. This space group affords no crystallographic special positions. The point group symmetry operators (xyz, $x\bar{y}\bar{z}$, $\bar{x}y\bar{z}$, $\bar{x}\bar{y}z$) therefore generate four magnetically distinguishable shielding tensors. With the cadmium in general position, the shielding tensor configuration must comply with C_1 site symmetry. Hence, four distinguishable tensors each with three distinct principal elements having general orientations with respect to the direction fo the three point group twofolds are indicated

Table XI. Direction Cosines Relating the Principal Shielding Directions of the ^{113}Cd Shielding Tensor to the Unit Cell Frame in the $Cd(OAc)_2 \cdot 2H_2O$ Crystal

tensor element,[a] ppm		direction cosines			angles, deg		
		a	*b*	*c*	*a*	*b*	*c*
σ_{11}	−118.7	−0.5899	0.3428	−0.7311	126	70	137
σ_{22}	−69.5	−0.5216	−0.8529	0.0210	121	148	89
σ_{33}	33.5	0.6164	−0.3937	−0.6820	52	113	133
$\bar{\sigma}$[b]	−51.6	$\eta = 0.58$					

[a] Chemical shifts are relative to solid $Cd(ClO_4)_2$. [b] $\bar{\sigma} = {}^1/_3(\sigma_{11} + \sigma_{22} + \sigma_{33})$.

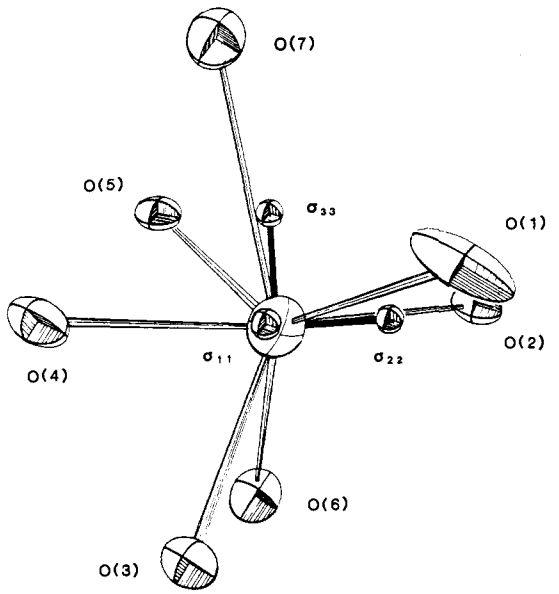

Figure 9. ORTEP of the ^{113}Cd shielding tensor orientation within the $Cd(OAc)_2 \cdot 2H_2O$ reference frame. O(1) and O(2) are water oxygens. O(3), O(4) and O(5), O(7) are bidentate acetate oxygens. The monodentate bridging acetate oxygen is O(6). The acetate carbons are not shown for clarity. The view is down the σ_{11}–Cd vector.

by symmetry. Four ^{113}Cd shielding tensors having the same principal moments but differing general orientations relative to the unit cell axes were determined. The principal elements of the shielding tensor and the set of direction cosines assigned to the molecular reference frame discussed below are given in Table XI.

The cadmium acetate reference frame is illustrated in Figure 9. Structural data are found in Table XII. Figure 9 shows cadmium to be seven-coordinate through two water oxygens, O(1) and O(2), two pairs of bidentate acetate oxygens, O(3) and O(4) and O(5) and O(7), and a monodentate bridging acetate oxygen, O(6). The Cd–O bonding distances range from 2.294 to 2.597 Å. Trotter and Harrison described the Cd-coordination geometry as a distorted square based–trigonal capped polyhedrons: O(1), O(2), O(3), and O(6) constitute the square base and O(4), O(5), and O(7) the trigonal cap. The structural features pertinent to this study are the cis orientation of the water oxygens in the square base and the angle (84°) that the longest bond, Cd–O(7), makes with the O(1), O(2), Cd plane.

Again referring to Figure 9, one finds the orientation of the ^{113}Cd shielding tensor to be dominated by the position of the water plane (O(1), O(2), Cd) and the direction of the longest bond, Cd–O(7). σ_{11} is directed 89° from the Cd–O(7) internuclear vector and 44° and 126° from the Cd–O(1) and Cd–O(2) vectors, with a resulting σ_{11}–water plane angle of 4°. Conversely, σ_{33} makes an angle of 9° with the Cd–O(7) vector and is directed 82° from the water plane. The σ_{33}–Cd–O(1) and σ_{33}–Cd–O(2) angles are 82° and 87°, respectively. The orthogonal orientation of the most shielded element with the longest Cd–O bond and the most deshielded element with the water plane is consistent with the eigenvalues ($\sigma_{11} = -118.5$, $\sigma_{33} = 33.5$ ppm). Further, σ_{22} is directed 81° from the Cd–O(7) vector and makes an acute angle

Table XII. Geometrical Data for $Cd(OAc)_2 \cdot 2H_2O$: Bond Distances and Angles for the Cd-Coordination Sphere and Tensor Element–Ligand Angles

bond distances, Å		bond angles, deg		tensor element–ligand angles, deg	
Cd–O(1)	2.299	O(1)–Cd–O(2)	83	σ_{11}–Cd–O(1)	44
Cd–O(2)	2.325	O(1)–Cd–O(3)	77	σ_{11}–Cd–O(2)	126
Cd–O(3)	2.546	O(1)–Cd–O(4)	91	σ_{11}–Cd–O(3)	48
Cd–O(4)	2.303	O(1)–Cd–O(5)	139	σ_{11}–Cd–O(4)	48
Cd–O(5)	2.294	O(1)–Cd–O(6)	136	σ_{11}–Cd–O(5)	130
Cd–O(6)	2.296	O(1)–Cd–O(7)	87	σ_{11}–Cd–O(6)	132
Cd–O(7)	2.597			σ_{11}–Cd–O(7)	89
		O(2)–Cd–O(3)	129		
		O(2)–Cd–O(4)	172	σ_{22}–Cd–O(1)	132
		O(2)–Cd–O(5)	92	σ_{22}–Cd–O(2)	143
		O(2)–Cd–O(6)	78	σ_{22}–Cd–O(3)	76
		O(2)–Cd–O(7)	95	σ_{22}–Cd–O(4)	42
				σ_{22}–Cd–O(5)	57
		O(7)–Cd–O(3)	130	σ_{22}–Cd–O(6)	79
		O(7)–Cd–O(4)	80	σ_{22}–Cd–O(7)	81
		O(7)–Cd–O(5)	53		
		O(7)–Cd–O(6)	134	σ_{33}–Cd–O(1)	82
				σ_{33}–Cd–O(2)	87
		O(3)–Cd–O(4)	54	σ_{33}–Cd–O(3)	134
		O(3)–Cd–O(5)	133	σ_{33}–Cd–O(4)	87
		O(3)–Cd–O(6)	85	σ_{33}–Cd–O(5)	57
				σ_{33}–Cd–O(6)	135
		O(4)–Cd–O(5)	90	σ_{33}–Cd–O(7)	9
		O(4)–Cd–O(6)	110		
		O(5)–Cd–O(6)	82		
		O(6)–Cd–O(7)	134		

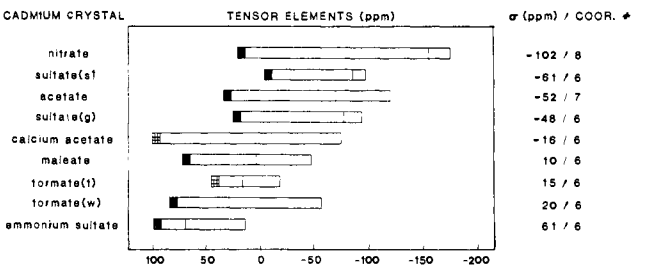

Figure 10. Summary of the ^{113}Cd shielding tensors for oxocadmium compounds determined by single-crystal experiments. Vertical bars represent the position of individual elements relative to $\bar{\sigma}$ for solid $Cd(ClO_4)_2$. The deshielded element of each tensor is designated by either a cross-hatched or a solid bar. Solid bars represent elements with intramolecular shielding contributions dominated by water oxygens. Cross-hatched elements indicate predominant short-bond shielding contributions. See the text for details. The nitrate and sulfate data is from previously reported work.[11] Sulfate suffixes correspond to cadmium in general and special positions.

of 7° with the O(1), O(2), Cd plane. The more general orientation of σ_{22} (−69.5 ppm) relative to the two structural features is in good agreement with the intermediate eigenvalue. The similarity between the tensor orientations in this case and in the unambiguous maleate should be noted.

Finally, Bryant and co-workers[35] have recently determined a different tensor–molecular reference frame orientation which places the most shielded element in an orthogonal direction relative to the cadmium–water oxygen plane. The eigenvectors for the two tensors are essentially related by the twofold along *c*. We are currently pursuing the ^{113}Cd–^{13}C dipolar couplings in ^{13}C-labeled cadmium acetate crystals to resolve this discrepancy.

Summary. Figure 10 provides a tabulation of the ^{113}Cd shielding tensors determined for oxo cadmium crystals. The crystals are listed in order of decreasing shielding, with the deshielded elements accentuated by broadened vertical bars. Several features should be noted. The deshielded elements span a range of 104 ppm (+100 to −4 ppm) while the shielded elements have nearly twice the shift

(35) Bryant, R. G.; Ganapathy, S., personal communication.

range, from −174 ppm for cadmium nitrate to 13.7 ppm for the cadmium Tutton salt. It is interesting that the intermediate elements show the largest shift dispersion of 224 ppm (−154 to +70 ppm). Finally, in all tensors studied, the deshielded elements reflect dominant shielding contributions either from Cd–HO_2 bonds (solid marks) or from short Cd–O bonds (cross-hatched). The concomitant long-bond–shielding correlations are also evident.

Conclusion

The tensor–molecular reference frame orientation has been determined for six distinct ^{113}Cd shielding tensors. The tensor orientations corresponding to the cadmium calcium tetraacetate and cadmium maleate crystals were unambiguously determined by NMR and crystallographic data. A simple method for assigning symmetry-related tensors to the appropriate lattice sites was introduced and employed in the analysis of the cadmium acetate, formate, and diammonium disulfate crystals. Three tensor element–structure correlations have been clearly demonstrated. First, the least shielded tensor element is aligned nearly perpendicular to the plane containing water oxygens. Second, if the coordination sphere is devoid of water oxygens, then the deshielded element is oriented to maximize the short-bond oxygen shielding contribution. Third, the shielded tensor element is directed nearly perpendicular to the longest cadmium–oxygen bond. With single-crystal NMR data for nine distinct tensors in seven different crystals these orientational features appear to be general.

To final comments are required. First, all tensor configurations have been found to comply with the cadmium site symmetry. Hence, the potential for significant intermolecular shielding contributions must be noted. The single-crystal data reported here will provide the opportunity to evaluate the magnitude of the intermolecular shielding contributions to the ^{113}Cd nucleus. Second, as mentioned above, a motivation for this work is an understanding of the characteristic shielding of the resonances corresponding to Cd-substituted parvalbumin,[3] troponin C,[4] calmodulin,[5] insulin,[6] and concanavalin A.[7] The nitrate, suflate, and acetate crystals have shielding tensor elements in the biological range of −85 to −130 ppm (Figure 10). In each case the shielded elements reflect major contributions from long Cd–O bonds. Further, the only isotropic shift in this region corresponds to the 8-coordinate cadmium nitrate. Clearly, one would not expect nitrate ligands to be involved in the Cd-coordination sphere of substituted metalloproteins. However, these data do suggest the following. The isolated closed-shell Cd(II) ion is the most shielded species possible. Any perturbation of this configuration via bond formation results in a deshileding of the cadmium nucleus. Hence poor ligands, i.e., nitrate and sulfate, and long Cd–O bonds indicate weak bonding interactions and are readily understood to be a shielding influence. With this in mind, the nitrate shift may be a reflection of ligand type as much as the higher coordination number. Similarly, the inability to produce model compounds with ^{113}Cd chemical shifts in the biolobical region may reflect a preoccupation with coordination number at the expense of ligand type. Consequently, we are currently pursuing compounds with carbonyl and hydroxide oxygens as ligands.

Acknowledgment. The authors thank Professor C. A. Hare for kindly supplying the atomic coordinates for $CdCa(OAc)_4 \cdot 6H_2O$ and Professor R. G. Bryant for sharing the cadmium acetate data prior to publication. R.S.H. acknowledges Dr. L. Lebioda for many helpful discussions during the preparation of this work. Further, we are grateful to Professor E. L. Amma for providing access to the necessary diffraction equipment. This work was supported in part by the National Institutes of Health (Grant GM 26295) and profited from use of facilities at the University of South Carolina National Science Foundation Regional NMR Center (CHE 82-07445).

Registry No. ^{113}Cd, 14336-66-4; $CdCa(OAc)_4 \cdot 6H_2O$, 27923-94-0; $Cd(O_2CHCCHCO_2) \cdot 2H_2O$, 26266-36-4; $Cd(OAc)_2 \cdot 2H_2O$, 5743-04-4; $Cd(NH_4)_2(SO_4)2 \cdot 6H_2O$, 14767-05-6; $Cd_2(HCO_2)_4 \cdot 4H_2O$, 51006-62-3.

Macrocyclic Dioxo Pentaamines: Novel Ligands for 1:1 Ni(II)–O_2 Adduct Formation

Eiichi Kimura,*[1a] Ryosuke Machida,[1a] and Mutsuo Kodama[2b]

Contribution from the Department of Medicinal Chemistry, Hiroshima University School of Medicine, Kasumi, Minami-Ku, Hiroshima 734, Japan, and Department of Chemistry, College of General Education, Hirosaki University, Bunkyo, Hirosaki 036, Japan.
Received January 26, 1984

Abstract: Substituted and unsubstituted macrocyclic dioxo pentaamines, 1,4,7,10,13-pentaazacyclohexadecane-14,16-dione, form stable 1:1 square-pyramidal complexes with Ni(II) and Cu(II), which possess two deprotonated amide donors in equatorial positions. The high-spin Ni(II) complexes show a very low Ni(II,III) redox potential of +0.24 V vs. SCE and are easily oxidized chemically or electrochemically to Ni(III) complexes. Moreover, the Ni(II) complexes react with molecular oxygen to form 1:1 Ni(II)–O_2 adducts in aqueous solution, as established by a combination of polarographic, spectrophotometric, and manometric methods. Comparative studies with relevant pentadentate macrocyclic polyamine complexes revealed that the two deprotonated amide groups and the fifth amine donor incorporated in the 16-membered macrocyclic frame are essential for the formation of the Ni(II)–O_2 adducts. The oxygen uptake reaction is first order in $[O_2]$ and in $[NiH_{-2}L]^0$ in aqueous solutions, and the second-order rate constant is 1.7×10^2 s^{-1} M^{-1} at 35 °C. The attack of O_2 at the sixth coordinate site is competitively inhibited by imidazole. The O_2 complexation constant K_{O_2} is determined to be 1.9×10^4 M^{-1} at 35 °C by potentiometric titration. Novel features of the Ni(II)–O_2 adducts are discussed.

The dioxo tetraamines depicted in Figure 1 posess the novel ligand properties of both saturated macrocyclic tetraamines (N_4) and oligopeptides.[2–6] They can accommodate certain metal ions Cu^{2+}, Ni^{2+}, Co^{2+}, and Pd^{2+}, within the macrocyclic N_4 cavities with simultaneous dissociation of the two amide protons (like tripeptides) to afford 1:1 complexes generally designated as $[M^{II}H_{-2}L]^0$. Peptide complex features of the coordinated imide

(1) (a) Hiroshima University. (b) Hirosaki University.
(2) Kodama, M.; Kimura, E. *J. Chem. Soc., Dlaton Trans.* **1979**, 325.
(3) Kodama, M.; Kimura, E. *J. Chem. Soc., Dalton Trans.* **1979**, 1783.
(4) Ishizu, K.; Hirai, J.; Kodama, M.; Kimura, E. *Chem. Lett.* **1979**, 1045.
(5) Kodama, M.; Kimura, E. *J. Chem. Soc., Dalton Trans.* **1981**, 694.
(6) Machida, R.; Kimura, E.; Kodama, M. *Inorg. Chem.* **1983**, *22*, 2055.

0002-7863/84/1506-5497$01.50/0